Specific Potassium Ion Interactions Facilitate Homocysteine Binding to Betaine-Homocysteine *S*-Methyltransferase

Jana Mládková[‡], Jana Hladílková[‡], Carrie E. Diamond[§], Katherine Tryon[§], Kazuhiro Yamada[¶], Timothy A. Garrow[§], Pavel Jungwirth[‡], Markos Koutmos[¶] and Jiří Jiráček[‡*]

Short title: Activation of BHMT by potassium ion

Keywords: BHMT; homocysteine; potassium; crystal structure; molecular dynamics; simulations; enzyme kinetics.

[‡] Institute of Organic Chemistry and Biochemistry, Academy of Sciences of the Czech Republic, v.v.i., Flemingovo nám. 2, 166 10 Prague 6, Czech Republic

[§] Department of Food Science and Human Nutrition, University of Illinois, Urbana, Illinois 61801, USA

[¶] Department of Biochemistry and Molecular Biology, Uniformed Services University of the Health Sciences, Bethesda, Maryland 20814, USA

[*] To whom correspondence may be addressed: Jiří Jiráček, Institute of Organic Chemistry and Biochemistry, Academy of Sciences of the Czech Republic, v.v.i., Flemingovo nám. 2, 166 10 Prague 6, Czech Republic. Tel.: 420-220-183-441; Fax: 420-220-183-571, E-mail: jiracek@uochb.cas.cz, or to tagarrow@illinois.edu (T.A.G., for biochemistry), pavel.jungwirth@marge.uochb.cas.cz (P.J., for theoretical experiments) and markos.koutmos@usuhs.edu (M.K., for X-ray crystallography).

ABSTRACT

Betaine-homocysteine *S*-methyltransferase (BHMT) is a zinc-dependent methyltransferase that uses betaine as the methyl donor for the remethylation of homocysteine to form methionine. This reaction supports S-adenosylmethionine biosynthesis, which is required for hundreds of methylation reactions in humans. Herein we report that BHMT is activated by potassium ions with an apparent K_M for K^+ of about 100 μM. The presence of potassium ions lowers the apparent K_M of the enzyme for homocysteine, but it does not affect the apparent K_M for betaine or the apparent k_{cat} for either substrate. We employed molecular dynamics (MD) simulations to theoretically predict and protein crystallography to experimentally localize the binding site(s) for potassium ion(s). Simulations predicted that K^+ ion would interact with residues Asp26 and/or Glu159. Our crystal structure of BHMT bound to homocysteine confirms these sites of interaction and reveals further contacts between K^+ ion and BHMT residues Gly27, Gln72, Gln247 and Gly298. The potassium binding residues in BHMT partially overlap with the previously identified DGG (Asp26-Gly27-Gly28) fingerprint in the Pfam 02574 group of methyltransferases. Subsequent biochemical characterization of several site-specific BHMT mutants confirmed the results obtained by the MD simulations and crystallographic data. Together, the data herein indicate that the role of potassium ions in BHMT is structural and that potassium ion facilitates the specific binding of homocysteine to the active site of the enzyme.

INTRODUCTION

Betaine-homocysteine *S*-methyltransferase (BHMT; EC 2.1.1.5) is abundant in the liver and kidney of monogastric animals.[1] It methylates homocysteine (Hcy) to regenerate methionine using betaine as the methyl donor. A constant supply of methionine is critical for the generation of *S*-adenosylmethionine, which is required for over 200 methylation reactions.[2] Betaine is an intermediate of choline oxidation and also functions as an organic osmolyte. BHMT expression is affected by dietary choline, betaine and methionine,[3,4] as well as other dietary factors such as sodium that influence cellular tonicity.[5,6]

Early work by Fromm and Nordlie[7] and Finkelstein et al[8] indicated that BHMT catalyzes a sequential reaction that proceeds by an ordered bi bi mechanism; Hcy is the first substrate on, and methionine the last product off. However, over the last 15 years much more information has been gathered about the kinetic and physical properties of BHMT. After the first full-length cDNA encoding BHMT was cloned,[9] and the recombinant protein was over-expressed in *E. coli* and purified to homogeneity,[10,11] ample amounts of human enzyme became available for detailed structure-function studies. BHMT was shown to contain a catalytic zinc (Zn) atom[10] while Cys247, Cys299 and Cys300 are required for Zn binding.[11,12] These biochemical findings were later confirmed by the crystal structure of human BHMT solved[13] in complex with the dual substrate inhibitor, *S*-(δ-carboxybutyl)-L-homocysteine (CBHcy, supplemental Chart S1).[14] These studies, as well as those conducted with folate- and cobalamin-dependent methionine synthase,[15,16] defined a new Zn binding motif and confirmed that BHMT and the Pfam 02574 group of enzymes methylate thiols via a Zn-tetrathiolate intermediate. Based on the BHMT:CBHcy crystal structure,[13] the enzyme is a tetramer and the primary fold of each monomer is a $(\alpha/\beta)_8$ barrel that contains an active site. With respect to substrate binding, the

backbone amide groups of Phe29 and Val30, and the γ-carboxyl of Glu159 are involved in Hcy binding, and the Phe76, Tyr77, Tyr160 and Trp44 are important determinants of the betaine binding site. Ligand binding studies and initial rate kinetics of selected mutants[17] support the role of Glu159 in Hcy binding, and indicate that Trp44 and Tyr160 are important betaine binding residues. Castro et al[17] also confirmed the bi bi reaction mechanism by showing that the betaine binding site is created following a conformational change triggered by Hcy binding. Immediately following the work of Castro et al,[17] the crystal structure of rat liver BHMT (free enzyme) was solved by Gonzalez et al.[18] This seminal contribution confirmed that most of the C-terminal residues that were originally unresolved in the human BHMT crystal structure are important for mutual binding of dimers and formation of a tetrameric unit. Additionally, by comparing the ligand-free rat enzyme[18] and human enzyme complexed with CBHcy inhibitor[13] structures, changes in the position of key BHMT residues during binding of the ligand can be accessed. Interestingly, in the rat BHMT structure, Tyr160 is the fourth ligand coordinating to Zn prior to Hcy binding, but in the human BHMT-CBHcy structure this residue is interacting with the carboxylate of the betaine mimic. Similarly, the locations of Phe76 and Tyr77 in the free and CBHcy-complexed enzyme are considerably different. Gonzalez et al[18] proposed that Phe76 and Tyr77 are initially involved in orientating Hcy for binding and then trigger a conformational change that creates the betaine binding site, which comes to include Tyr160, Phe76 and Tyr77, among other residues. These studies, as well as a series of papers that have tested novel inhibitors of BHMT to investigate the tolerance of the enzyme toward substrate functional group modifications,[14,19,20] have provided considerable detail to our understanding of BHMT structure and function including its exquisite selectivity for Hcy.

With respect to the remarkable selectivity BHMT has for L-Hcy, the results reported herein show that potassium ion has a structural role in BHMT and that it stimulates BHMT activity by facilitating Hcy binding. The stimulation of BHMT activity by potassium ions was identified by enzyme kinetics experiments. The potassium ion-binding site was predicted by MD simulations and solved by X-ray crystallography independently. Mutant BHMT enzymes were studied using initial rate kinetics and ligand binding assays to verify the data obtained by MD simulations and X-ray crystallography. The potassium binding site in BHMT is composed of Asp26, Glu159, Gly27, Gln72, Gln247 and Gly298 residues and its location is identical to that in methionine synthase (MS) from *T. maritima*.[21] Moreover, BHMT potassium binding site residues partially overlap with the previously identified DGG (Asp26-Gly27-Gly28) fingerprint[11,13] in the Pfam 02574 group of methyltransferases.

MATERIALS AND METHODS

Materials.

Unless otherwise stated, reagents and materials were obtained from commercial suppliers (Sigma-Aldrich, Fisher, Fluka, Merck) and used without purification.

Synthesis of *S*-[methyl-^{14}C]methyl-L-methionine chloride.

S-[methyl-^{14}C]methyl-L-methionine chloride (^{14}C-SMM) was prepared, characterized and stored as described previously.[22]

Cloning of mutated variants of BHMT.

Site-directed mutagenesis of BHMT was performed using a QuikChange II kit (Stratagene) with primers designed using the manufacturer's web-based primer design program and pTYB4-hBHMT as the template. All mutations were verified by DNA sequencing.

Expression and purification of human BHMT and its mutants.

Wild-type (WT) and BHMT mutants were purified as described previously[11] with several modifications. In brief, 30 mL of 2xYT media containing 0.1 mg/mL ampicillin was inoculated with a culture of *E. coli* BL21(DE3) cells transformed with pTYB4-hBHMT plasmids. After growing the cells (37 °C) to A_{595}=0.6, the cells were collected by centrifugation (1,500 g, 10 min) and used to inoculate 1 L of 2xYT media containing 250 μM zinc chloride and 0.1 mg/mL ampicillin. The 1 L cultures were grown (37 °C) until A_{595}=1 and then induced with IPTG (0.3 mM, Duchefa Biochemie B.V.) and incubated for a minimum of 16 hours. Following the induction period, the cells were collected by centrifugation at 4,500 g for 10 min (4°C) and resuspended in 20 mL of cold 20 mM Tris/HCl buffer (pH 8.0) containing 0.5 M NaCl, 0.1 mM EDTA, 0.1% Triton X-100 (w/v). Then, Protease Inhibitor Cocktail Set I (Calbiochem) and about 5 mg of TCEP (Sigma) and about 5 mg of DNAse I (Sigma) were added to the cells, which were then lysed using a French press. The extract was then sonicated to shear the cellular DNA. The lysate was centrifuged (22,500 g, 90 min, 4°C) and the enzyme purified at 4°C using chitin affinity chromatography (Chitin Beads, New England Biolabs). The chitin affinity column (20 mL) was washed with 200 mL of MilliQ water and then equilibrated with 200 mL of 20 mM Tris/HCl (pH 8.0) buffer containing, 0.5 M NaCl, 0.1 mM EDTA, 0.1% Triton X-100 (w/v) and 0.2 mM TCEP. The lysate was supplemented with about 5 mg of DNAse I and then applied to the column (0.5 mL/min). The column was washed (1 mL/min) with 600 mL of the same buffer and then 100 mL of buffer containing 20 mM Tris/HCl (pH 8.0), 50 mM NaCl, 0.1 mM EDTA, 0.2 mM TCEP and 10% glycerol (w/v), and finally rapidly (5 mL/min) with 30 mL of the same buffer supplemented with 30 mM β-mercaptoethanol. The column was then allowed to stand for a minimum of 16 hours at 4°C. Afterwards, proteins were eluted using 20 mM Tris/HCl (pH 8.0) buffer containing 50 mM NaCl, 0.1 mM EDTA, 0.2 mM TCEP, 10% glycerol (w/v) and 30 mM

β-mercaptoethanol. The protein concentration was determined using the Bradford assay.[23] Protein purity and identity was confirmed by SDS-PAGE and MS analysis of tryptic digests as described previously by Mladkova et al.[22]

BHMT activity assays.

BHMT activity using betaine as the methyl donor was assayed as previously described.[19] N-methyl-^{14}C-betaine (57 mCi/mmol) was prepared and supplied by Moravek Biochemicals (Brea, CA). The standard reaction mixture (0.5 mL) contained 250 μM betaine (0.3 μCi), 100 μM D,L-Hcy, 50 mM Tris/HCl (pH 7.5), 0.07% (w/v) β-mercaptoethanol and 0.2 μM BHMT. The concentration of substrates (betaine and D,L-Hcy) varied in different experiments when Michaelis-Menten constants were measured as indicated in the figure legends but the rest of the conditions was the same as in the standard reaction mixture.

The standard reaction mixture (0.2 mL) using *S*-[methyl]methyl-L-methionine (SMM) as the methyl donor contained 0.25 mM SMM (0.3 μCi ^{14}C-SMM), 2.5 mM D,L-Hcy, 50 mM Tris/HCl (pH 7.5), 0.1% (w/v) β-mercaptoethanol and 0.2 μM BHMT. D,L-Hcy, kept under nitrogen, was freshly dissolved in 50 mM Tris/HCl (pH 7.5) and immediately used in the assay. Reaction tubes were kept in ice-cold water until the assay was started by transferring the tubes into a 37°C water bath. After 60 min, the reaction was stopped by transferring the tubes into ice-cold water. Then, 1.5 mL of methanol was added to tube and reaction mixture centrifuged (16,000 g, 5 min, 4°C). Supernatants were applied to Dowex 1x4 (OH^-; 200-400 mesh) columns (1 mL of resin). Unreacted SMM was washed from the column with water (3 x 5 mL) and methionine product was eluted into vials with 1.5 M HCl (1.5 mL). Then, scintillation cocktail (10 mL) was added to each vial and counted. Blank tubes contained all of the reaction components except enzyme, and their values were subtracted from the sample values. All samples were assayed at least in triplicate. The concentration of substrates (SMM and D,L-Hcy) varied in different experiments

when Michaelis-Menten constants were measured as indicated in the figure legends but the rest of the conditions was the same as in the standard reaction mixture.

The data were analyzed using the GraphPad Prism 5 program (GraphPad Software, Inc.) with nonlinear regression fit and apparent K_M (± S.E.) values were calculated from three independent measurements with all points in tetraplicates.

Measurement of Hcy binding by changes in steady-state intrinsic fluorescence.

Changes in the steady-state intrinsic fluorescence of BHMT where measured holding dimethylglycine constant (1 mM) at saturating levels while L-Hcy was varied to determine the ternary dissociation constant (K_d) with limiting L-Hcy. The procedures have been previously described in detail.[17] These experiments were done in 50 mM Tris/HCl (pH 7.5) buffer, but the L-Hcy was prepared using a saturated KH_2PO_4 solution to neutralize the NaOH-stimulated conversion of L-Hcy-thiolactone to L-Hcy. Thus, the final concentration of potassium ions in the reaction mixture was approximately 10 mM.

Computational methods.

From the tetrameric ligand-depleted BHMT crystal structure (PDB accession number 1UMY)[18] we selected the monomer (chain D) together with the dimeric (chain C) and the tetrameric (chain B) clipping parts, which are the essential parts for formation of the active enzyme. In total 412 amino acids and a single zinc ion were solvated in ~14,600 water molecules. These include both water molecules from the crystal structure and additional bulk liquid water molecules. There are two different approaches in the literature regarding how to simulate enzymes with a transition metal zinc ion. The first one treats it similarly to a calcium dication with no charge transfer from the surrounding active site,[24] while the second one uses charges estimated from quantum chemistry calculations.[25] We chose to apply both of these methods and compare the results. We used the natural population analysis as implemented in the Gaussian 09

package[26] for *ab initio* calculation of charges in the active site and considered both possibilities for the protonation state of Cys300[27] (the commentary is in the Supporting Information). The total charge of the whole enzyme of +3e for the protonated cysteine was compensated by counterions (i.e., 3 chloride ions), on top of which we added 0.16 M chloride salts (i.e., 42 molecules of NaCl, KCl, or RbCl). The parameterization of Na^+, K^+, Rb^+ and Cl^- was the same as in our earlier studies,[28,29] which proved to be a reliable choice in combination with the AMBER ff03 protein force field[30] and the SPC/E water model.[31]

For simulations of the BHMT monomer with the CBHcy inhibitor in the active site (PDB accession number 1LT8)[13] we recalculated the amount of charge transfer to the zinc cation as the inhibitor coordinates with the zinc as one of its ligands. The simulation protocol was the same as described below, but the residues at and around the inhibitor site were enabled to move freely.

MD simulations were performed using the Amber 11 program package.[32] Potential energy of the system was first minimized with constrained positions of protein atoms using the steepest descent method in order to avoid energetically unfavorable close contacts.[33] The system with constrained protein was then heated up to 315 K corresponding to the experimental conditions, with volume held fixed and then pressure coupling was used to reach the equilibrium density at 1 atm. 3D Periodic boundary conditions were applied to the system with a unit cell size of 80x80x80 $Å^3$. Equilibration lasted for 2 ns and the data were then collected from 350 ns production runs for each of the simulated system. All bonds containing hydrogens were constrained using the SHAKE algorithm,[34] allowing for a 2 fs time step for all the simulations. The short range non-bonded interactions were cut off at 8 Å and smooth particle mesh Ewald (PME) method accounted for the long range electrostatic effects.[35] The pressure and temperature of the system were regulated by the Berendsen´s barostat and termostat.[36]

Analysis of the simulation data was based on ion density map calculations.[28] The regions where ions occur with a higher probability than in the bulk solution were visualized. Ion maps gave us a qualitative answer concerning the most probable spots for ion binding. For quantitative comparison, we needed to use an additional analytical tool, namely the radial distribution function. To this end, radial distribution functions (i.e., probabilities of ions to occur at a certain distance from a defined center) were integrated yielding numbers of ions within a specified region.

Protein crystallization.

Crystals of wild type human BHMT with L-Hcy were prepared as follows. Crystals were grown at 4 °C under oil in microbatch trays by mixing 2 µL of 11mg/ml protein in 50mM Tris/HCl, pH 8.0, 1 mM TCEP, and 20 mM L-Hcy with 2 µl of solution containing 20.0% PEG 5000 MME, 0.2 M sodium/potassium tartrate, and 0.4 µl of 15% 1,2,3-heptanetriol. Crystals were cryoprotected by transfer to a solution of 22% PEG 5000MME, 0.2 M sodium/ potassium tartrate, 16% propylene glycol, 20mM L-Hcy and 50 mM Tris/HCl pH 7.5. Crystals of BHMT with L-Hcy were of space group $P2_1$ (a = 86.1, b = 102.6, c = 96.2, β = 106.3) with 1 BHMT tetramer in the asymmetric unit (Matthews' coefficient, V_M = 2.3 $Å^3$/Da for 4 BMHT monomers, 46.8% solvent content).

L-Hcy was prepared as follows. 150 mg of L-Hcy thiolactone were dissolved in 5 ml water. 2.5 ml of 0.8 M NaOH were added, followed by degassing with argon for 5 minutes, and incubation for 6 min at 45 °C. ~2.5 ml of 0.4 M acetic acid were then added to reach pH 5. Aliquots were stored under argon at -80 °C. Fresh aliquots were used for every crystallization and the concentration was measured by determining the thiol content through a 5,5'-dithio-bis(2-nitrobenzoic acid) (DTNB) assay as previously described.[37]

Data collection, structure determination and refinement.

Diffraction data were collected at GM/CA-CAT IDD (Advanced Photon Source, Argonne National Laboratory) on a Mar 300 detector and processed with XDS[38] to 1.9 Å resolution. Initial phases were obtained by the molecular replacement (MR) method with EPMR[39] using the coordinates of human BHMT complexed with CBHcy inhibitor[13] (PDB accession number 1LT8) as a search model. For the search model we utilized just the $(\alpha/\beta)_8$ barrel while we omitted all the connecting loops, the CBHcy ligand, Zn and water atoms. Initial density allowed for ligands and metal ions to be added. The BHMT:L-Hcy structure was refined with CNS,[40] including rigid body refinement of the individual domains followed by simulated annealing in torsional and Cartesian space, coordination minimization, and restrained individual B-factor adjustment with maximum-likelihood targets. Refmac5[41] of the CCP4 suite[42] was subsequently employed for restrained refinement of using isotropic individual B-factors with maximum-likelihood targets, using the Babinet model for bulk solvent scaling, followed by model building and modification with Coot.[43] Several iterative rounds of refinement followed by model building/modifications were performed. In early rounds of refinement with CNS, restraints for the bound L-Hcy, and ideal targets for tetrahedral geometry at zinc were added. The latter were however removed upon subsequent model refinements with Refmac5. A large positive electron density in the vicinity of the carboxy-amido part of the bound L-Hcy ligand was later on modeled and refined with a K^+ atom. Crystallographic information as well as refinement statistics are provided in the supplemental Table S1. The geometric quality of the model and its agreement with the structure factors were assessed with MolProbity.[44] For BHMT:L-Hcy, MolProbity reported a clash and a molprobity score of 2.27 (99^{th} percentile) and 1.45 (97^{th} percentile) respectively, while 97.0% of

the residues were in the favored Ramachandran plot regions with 2 outliers (0.14%) Figures showing crystal structures were generated with PyMOL (The PyMOL Molecular Graphics System, Version 1.3r1, Schrödinger, LLC, 2010).

RESULTS

Dependence of BHMT activity on potassium ions.

The influence of monovalent cations on BHMT activity was studied in detail. Among the monovalent cations investigated (Li^+, Na^+, K^+, Rb^+, Cs^+ and NH_4^+; all cations at 0 - 400 mM concentration), K^+ was the only cation that significantly stimulated BHMT activity. BHMT activity displayed a Michaelis-Menten type behavior with increasing K^+ concentrations and an apparent K_M for K^+ of about 100 μM (Figure 1, in a logarithmic scale). The presence of 150 mM Rb^+ or NH_4^+ only marginally stimulated BHMT activity, while the same concentrations of Li^+, Na^+ and Cs^+ had negligible impact. However, all the tested monovalent cations inhibit BHMT activity at high concentrations (> 300 mM) (Figure 1). The stimulatory effect of K^+ was not affected by the nature of the counter ion since both Cl^- or Br^- salts were equally effective (data not shown).

Previous studies have reported significantly different K_M values of BHMT for betaine and Hcy.[10,45,46] K_M values for betaine range from 100 μM to 2.2 mM, and K_M values for Hcy range from 4 μM to 120 μM. These values were determined using different buffering agents and different concentrations and sources of K^+. Because of the effect of K^+ on BHMT activity, we reinvestigated the initial rate kinetics of BHMT using a Tris/HCl buffer containing 150 mM KCl. This potassium ion concentration not only gives rise to the maximum stimulatory effect on BHMT activity (Figure 1), but it also corresponds to the physiological levels of potassium in the

cell.[47] Using these buffer conditions, we determined that the K_M values for betaine and D,L-Hcy are about 60 μM and 15 μM, respectively. The K_M values for betaine and D,L-Hcy measured in Tris/HCl buffer devoid of potassium ions were about 75 μM and 338 μM, respectively (Table I and supplemental Figure S1AB). Individual k_{cat} values for the respective reactions, when either betaine or Hcy were the varied substrate, were similar and ranged from 107 to 152 h^{-1}.

By contrast, no BHMT activity was detected when SMM and Hcy were used as substrates in Tris/HCl buffer devoid of potassium ions. Moreover, with the exception of potassium ions, no other monovalent cations were able to stimulate SMM-dependent BHMT activity. Thus, BHMT is able to use SMM as a substrate only when K^+ ions are present (supplemental Figure S2). The K_M values of BHMT for D,L-Hcy and SMM measured in Tris/HCl buffer with 150 mM KCl were approximately 2.3 mM and 3.4 mM, while k_{cat} values were approximately 1.2 and 16 h^{-1}, respectively (Table I and supplemental Figure S3). However, it is important to note that measuring apparent K_M and k_{cat} values for SMM and Hcy was possible only in a limited range of substrate concentrations because concentrations of D,L-Hcy above 10 mM and concentrations of SMM above 4.5 mM led to decreased activities (data not shown). Therefore, we were not able to reach the maximum velocity and all kinetics constants are presented as approximate (as indicated in Table I with the sign "~").

Molecular dynamics (MD) simulations.

Following the experimental characterization of BHMT activity in the presence and absence of monovalent cations, theoretical calculations were initiated in order to predict the nature of the potassium ion(s) binding site(s) within BHMT. After collecting all data from the MD production runs, ion density maps, as well as radial distribution functions were constructed for the enzyme in three 0.16 M ionic solutions for NaCl, KCl, and RbCl. Ion density maps provided a visually clear answer about the ion distributions around the enzyme. Comparing ion maps for Na^+, K^+, and Rb^+,

we found out that the regions where ions reside with the highest probability are the same for all three ions. The potassium distribution around the enzyme, with an isovalue corresponding to concentration 10-fold higher than that in the bulk, is displayed in Figure 2. Globally, the ion binding spots are located primarily close to the negatively charged residues (Asp and Glu) and the carbonyl groups of the protein backbone. For a more quantitative analysis we evaluated average numbers of ions located in the individual binding spots. Based on our previous work on a variety of enzymes[48] Na^+ binds more strongly to negatively charged residues than K^+ or Rb^+. BHMT generally follows this trend; nevertheless, we found two connected regions close to the active site where the ordering of the cations is different and in favor of K^+.

In Figure 2A, the active site of ligand-depleted BHMT enzyme with the zinc cation (grey) and its four ligands (yellow) is shown enlarged. Two major cationic binding sites are found close to the two negatively charged residues - Asp26 and Glu159 within a 9 Å radius from the zinc ion. The cumulative numbers of individual cations in this area and the corresponding radial distribution functions are presented in Figure 3. In Figure 3, we see that at these active site cationic binding spots the potassium ion binds the strongest, followed by rubidium ions, which is in agreement with experimental ordering of cations according to their enhancement of the enzymatic activity (Figure 1).

To check whether and how the binding site of potassium is affected by the presence of the substrate and/or inhibitor, we performed additional MD simulation with the bound CBHcy inhibitor. As it is evident in Figure 2B the potassium ion moves closer to Asp26 while the potassium binding site slightly rearranges to accommodate this shift. One of the two original potassium binding sites in the vicinity of Glu159 is now occupied by the inhibitor so only one binding site for potassium remains close to the active site. A detailed view of the structural changes at the potassium binding site predicted by our studies in the presence of the inhibitor is

provided in Figure 4. We also calculated the number of water molecules in the first solvation shell of Rb^+, Na^+, and K^+ (without and with the inhibitor) in the active site. The data (Figure S4) and a detailed commentary are provided in the Supporting Information; in a nutshell, we can say here that potassium accommodates best out of the three cations in the binding site.

Crystallography – BHMT:L-Hcy complex.

In parallel to theoretical MD calculations, we successfully crystallized and determined the crystal structure of tetrameric human BHMT in a complex with L-Hcy. The overall protein structure is shown in Figure 5. In contrast to our previous structure of human BHMT complexed with the specific inhibitor CBHcy,[13] we clearly detect a potassium atom at the active site of BHMT.

For our crystallization experiments, we utilized potassium salts in our crystallization buffers. In the resulting electron density maps based on the collected data of a BHMT with L-Hcy crystal, we clearly observe strong positive electron density in the vicinity of the carboxy-amino part of the Hcy ligand bound to Zn. In the calculated 2Fo-Fc weighted composite omit map for each monomer we observe two strong electron density peaks (> 8σ in the 2Fo-Fc maps) (Figure 6AB). The strongest peak (13σ), as displayed in the in Figure 6B, coincides with the expected Zn binding site and which was modeled and later refined as Zn while the second strongest peak (9σ), as displayed in Figure 6A, belongs to what we believe is the K^+ atom. If a water molecule is modeled instead of the potassium ion strong residual positive electron density peak is centered at this molecule position indicating the incorrect assignment with a "light" atom and the requirement of a "heavier" in that position.

The K^+ ion binding site (Figure 6CD) exhibits a coordination of 8 and average $K^{+\cdots}$ O distance of 2.9 Å (range 2.7 – 3.2 Å for all 4 K^+ sites in BHMT monomers). The K^+ ion binding site is assembled from residues Asp26, Gly27, Gln72, Gln247 and Gly298. The K^+ ion is positioned in a

shallow grove mainly formed by the three main chain carbonyl groups of residues Asp26, Gly27 and Gly298 (average $K^{+\cdots} O_{carbonyl}$ of 2.8 Å), while its coordination is completed by two amide O atoms of Gln72, Gln247 (average $K^{+\cdots} O_{amide}$ of 3.0 Å), one carboxylate O atom of Asp26 (average $K^{+\cdots} O_{carboxylate}$ of 2.8 Å) and two water molecules (average $K^{+\cdots} O_{water}$ of 2.9 Å).

The Hcy ligand bound to Zn^{2+} ion is found in a conformation similar to the one reported for CBHcy inhibitor, *S*-(δ-carboxybutyl)-homocysteine, bound to BHMT (PDB code 1LT8).[13] Hcy is anchored to the protein through additional interactions with Glu159 through its amino-group and with main chain amides of Phe29 and Val30 through its carboxy group. Interestingly, the K^+ binding site is proximal to the Hcy-binding site (Figure 6CD). Based on our new structure, the K^+ ion forms a water-mediated interaction with one of the carboxy O atoms of Hcy. Moreover, the Glu159 residue involved in Hcy binding forms also a water-mediated interaction with the K^+ ion.

BHMT mutants.

The results from the MD simulations and the crystal structure implicate residues Asp26, Glu159, Gly27, Gln72, Gln247 and Gly298 in the binding of potassium ions and/or Hcy. We previously discussed the potential importance of the Asp26-Gly27-Gly28 (DGG) fingerprint[13] and that mutating Glu159 to Gln inactivated enzyme activity.[17] Therefore, we made additional BHMT mutants at positions Asp26, Gly27, Gly28 and re-evaluated Glu159 to determine whether changes at these positions affected the ability of potassium to stimulate BHMT activity and/or affect Hcy binding. Gly27Ser and Gly28Ser mutants were prepared based on mouse variations at the BHMT-2 locus.[49] The purification yields and activities of the various mutants are listed in Table II.

Under the same purification conditions, Gly27Ser, and especially Glu159 mutants provided very low or zero yields. All the mutants were much less active than the WT enzyme. The only mutant that retained significant activity was Gly28Ser, and it was affected by potassium ions to a

similar extent as the WT enzyme. The Asp26Ala had very low activity compared to WT enzyme, whereas the Gly27Ser and all Glu159 mutants were completely inactive.

Additionally, we performed experiments to determine the dissociation constant of Hcy by measuring the formation of the BHMT-Hcy-dimethylgycine ternary complex using steady-state intrinsic fluorescence, as previously described.[17] These experiments held enzyme and dimethylglycine (1 mM; saturating) constant while the concentration of Hcy was varied. The buffer contained 10 mM potassium ions, which is the concentration sufficient for near maximum stimulatory effect of the ion (see above). The data in Table II show that the binding affinity of all the mutants for Hcy are severely reduced, i.e. no binding for Gly27Ser, 61 μM for Gly28Ser, and 116 μM for Asp26Ala, compared to 4 μM for WT BHMT.

The SDS-PAGE combined with MS analyses of tryptic digests confirmed the presence of highly pure wild type BHMT as well as BHMT mutants. The only distinction was in the case of preparation of Glu159Asp mutant where no protein was detected neither using Bradford assay nor SDS-PAGE (supplemental Figure S5). The experimentally determined relative molecular masses of recombinant BHMT were similar to their predicted masses of about 45 kDa.

DISCUSSION

BHMT and BHMT-2 share a high degree of amino acid identity, which suggests their substrate specificities might overlap. Szegedi et al[50] demonstrated that BHMT-2 can methylate Hcy using SMM but not betaine. They went on to show that BHMT can also use SMM instead of betaine as a methyl donor but with markedly reduced catalytic efficiency. However, more recently we observed that BHMT is not able to use SMM in a Tris/HCl buffer unless potassium ions were present.[22] This observation led us to examine the influence of potassium ions and other

monovalent cations on BHMT activity and substrate selectivity. To achieve this goal, we followed three parallel lines of the study; biochemical experiments, theoretical calculations, and crystallographic studies with BHMT.

Among the monovalent cations studied, only potassium ions had a strong stimulatory effect on BHMT activity and Rb^+ and NH_4^+ cations only barely stimulated enzyme activity while Li^+, Na^+ and Cs^+ had negligible impact (Figure 1). This is in a good agreement with previous studies that showed that enzymes that are stimulated by K^+ are also activated by Rb^+ and NH_4^+, but not activated by the larger (Cs^+) or smaller (Na^+ and Li^+) cations.[51]

The half maximal stimulation of BHMT by potassium ions is at about 100 μM and concentrations over 300 mM have an inhibitory effect. The decrease in activity observed when K^+ levels were over 300 mM is likely due to the increased ionic strength since the inhibition is caused also by salts other than KCl. It is known that the uptake of high K^+ concentrations has inhibitory effects for cells.[47] Therefore, it can be expected that BHMT is maximally active at normal intracellular concentrations (i.e., about 150 mM K^+).

The apparent K_M of the enzyme towards betaine is not significantly affected by potassium ions. However, the apparent K_M towards Hcy without KCl is about 20-times higher than the K_M measured at 150 mM KCl. In contrast, k_{cat} values did not significantly differ when potassium ion concentrations varied. These data (Table I) indicate that potassium ion most probably doesn't have a direct role in catalysis, but that it has an important structural role by facilitating and/or stabilizing Hcy binding.

We previously showed[22] that BHMT is unable to methylate Hcy using SMM, the substrate for the BHMT paralogue BHMT-2, in a buffer devoid of potassium ions. However, even at 150 mM KCl, the apparent values of K_M for SMM and Hcy are in the milimolar range and the respective

turnover numbers (k_{cat}) are also significantly lower than the values determined when betaine and Hcy are the substrates. It is thus unlikely that BHMT has any significant role in the metabolism of SMM even if high intracellular concentrations (> 2 mM) of this metabolite are present in the human liver as originally predicted by Szegedi et al.[50] This is consistent with *in vivo* studies that used SMM as a chemoprotective agent against acetaminophen (Tylenol) toxicity. In those studies, a downstream metabolite of methionine, glutathione, was only maintained in the liver of mice with normal BHMT-2 activity and not in those mice lacking BHMT-2 activity, even though the latter mice had normal levels of BHMT expression.[49]

Two independent approaches were undertaken to theoretically predict and experimentally determine the structural nature of potassium ions´ role in BHMT catalysis, MD simulations and X-ray crystallography, respectively.

For simulations, the crystal structure of rat BHMT (PDB code 1UMY)[18] was employed because it represents the structure of the native enzyme without any bound ligand. In parallel, calculations were also performed on the platform of human BHMT because in this structure (PDB code 1LT8) the enzyme is complexed with a specific inhibitor, CBHcy,[13] which acts as a transition-state or biproduct analogue.[19] The geometries of BHMT active sites in both crystal structures differ slightly because the binding of the inhibitor causes replacement of several residues, mainly Phe76, Tyr77 and Tyr160, which is the fourth ligand of the zinc in the ligand-depleted enzyme[18] and which is replaced by the sulfur atom of CBHcy when bound to the active site.[13]

MD simulations revealed regions with the highest probability of K^+ occurrence in the active site of BHMT. Two sites lined between Asp26 and Glu159 (Figure 2A) and one distinct site close to Asp26 (Figure 2B) were found in ligand-depleted enzyme and in CBHcy-complexed enzyme, respectively. Although Na^+ is known to usually bind more strongly to negatively charged

residues,[48] in BHMT active site potassium ions were predicted to bind most strongly (Figure 3). The results displayed in Figure 3 suggest that only one potassium cation may be present in the active site due to the charge compensation. These results suggested that one K^+ may oscillate between two carboxylic groups of both amino acids in the absence of any substrate or inhibitor. In CBHcy-bound enzyme, the density enhancement of K^+ occurs only at the "hotspot" closer to the carboxylate of Asp26 (Figure 2B). In our simulations, the carboxy amino moiety of the inhibitor is intercalated between the K^+ ion and the carboxylate of Glu159, which both clearly participate in the inhibitor stabilization in the active site. Based on our calculations, in the enzyme void of bound ligand four water molecules are predicted to hydrate the potassium ion. However, with CBHcy inhibitor bound, only two waters are bound to the ion (Figure S4). In contrast, sodium and rubidium cations switch frequently between full hydration and partial dehydration indicating that their position in the active site is more exchangeable than that of potassium ion. Overall, this theoretical model supports a structural role for potassium ions by increasing the binding affinity of Hcy for BHMT, which is the first substrate to bind,[17] while the affinity for betaine would be K^+-independent (values of K_M in Table I).

In parallel to the theoretical calculations, we performed crystallization trials to determine the structure of BHMT in a complex with Hcy in order to determine the location and assess the participation of potassium ions in Hcy binding. The potassium site identified in our X-ray crystal structure (Figure 5 and 6) was previously undetected at the equivalent site in the previously published structures.[13] Instead, it was incorrectly modeled as a water molecule. It is quite possible that in the previous structures this site was occupied by a K^+ ion with lower occupancy, which would render it almost indistinguishable from the nearby O and N atoms solely based on electron density considerations.

The high coordination number (eight) of K^+ ion observed in the crystal structure of BHMT complexed with Hcy is not surprising given the ability of K^+ ions to expand their coordination geometry to numbers greater than 6 and up to 9, while the most common coordination number for K^+ ions in small molecules is 8.[52] Moreover, the average $K^{+\cdots}$ O distance of 2.9 Å is in good agreement with the mean $K^{+\cdots}$ O distance of 2.84 Å found in other proteins.[52] The position and coordination of K^+ ion and overall structure of the active site of BHMT with Hcy bound as determined here by X-ray crystallography (Figure 6CD) are in a good agreement with results of MD simulations performed with a complex of BHMT with CBHcy inhibitor (Figure 4). Both methods have also revealed the presence of only two water molecules chelating the K^+ ion in BHMT with bound ligands (Figure 4, S4 and 6CD).

BHMT, BHMT-2, and cobalamin-dependent methionine synthase (MS) are the three enzymes in mammals that catalyze the conversion of Hcy to methionine. BHMT and MS enzymes utilize a $Zn(Cys)_3$ moiety to bind and activate Hcy in a similar fashion.[10,16] Despite the lack of structural information about BHMT-2, we may assume that the active site will be similar to BHMT and MS.

The two latest published MS structures[21] from *T. maritima* (PDB codes 3BOF and 3BOL) were crystallized also in the presence of K^+ ions, and similarly to the BHMT structure reported here, exhibit a previously undetected K^+ binding site (supplemental Figure S6). The location of the K^+ binding site in MS is identical to that in BHMT with the two sites superimposing perfectly. Furthermore, the architecture of the potassium ion binding site in MS is generally similar to that in BHMT. The K^+ ion in MS unlike BHMT exhibits a coordination number of 6 with an average $K^{+\cdots}$ O distance of ~2.8 Å (range 2.6 – 2.9 Å for all 4 K^+ sites found in the two MS structures). This distance is slightly shorter than the equivalent distance in BHMT and can perhaps be attributed to its lower coordination number. Similar to BHMT, the K^+ binding site in MS is

formed primarily by the main chain carbonyl groups of invariant residues Asp17, Gly20 and Gly271 which correspond ideally with the locations of Asp26, Gly27, and Gly298 in human BHMT (supplemental Figure S7). The coordination sphere of potassium ion in MS is completed by the carboxylate O atoms of Asp19 (Asp26 in human BHMT), and Glu232 (Gln247 in human BHMT) and one water molecule instead of two in human BHMT. While the two glycine and one aspartate ligands integral to the formation of the K^+ binding site are conserved among BHMT and MS there is more variability with respect to the other ligands that comprise the K^+ binding site. The equivalent position of Gln72 in human BHMT is occupied by Leu62 in *T. maritima* MS. The latter residue in mammalian or *E. coli* MS is replaced by a glutamate moiety, which would be in a position to interact with the K^+ ion in a manner similar to Gln72 in human BHMT, while Glu232 in *T. maritima* MS is replaced by a residue in mammalian or *E. coli* MS that would not be a suitable K^+ ligand. In other words, in MS despite the partial variability in the lining of the K^+ binding site the coordination number is predicted to be the same. Additionally, the Hcy ligand in MS is also in close proximity to the K^+ ion with the latter interacting with the amine Hcy group through a water molecule similar to what is observed in BHMT. Likewise, Hcy binding determinant Glu146 in *T. maritima* MS (Glu159 in human BHMT) forms a water-mediated interaction with the K^+ ion.

We cannot fully exclude that the apparent proximity and coupling of the K^+ ion to the bound Hcy ligand may have some functional implications in the chemistry of the reaction of both BHMT and MS enzymes because rate limiting steps in the catalytic reactions of these enzymes are not known. However, the findings that the presence of potassium ions lowers the apparent K_M of BHMT for Hcy only, but it does not affect the K_M for betaine neither k_{cat} values for either of the substrates (Table I), convincingly suggest the exclusive structural role of K^+ ion in facilitating Hcy binding and not in the catalytic reaction of BHMT.

The results obtained by MD simulations and X-ray crystallography encouraged us to perform experiments with selected BHMT mutants to confirm the role of key residues implicated in potassium, and by extension, Hcy binding. Among the mutants studied (Table II), only Gly28Ser displayed moderate but significant activity for betaine and Hcy substrates. All other mutants gave either very low activities (Asp26Ala and Gly27Ser) or non-detectable activities (all Glu159 mutants). Additionally, the Gly28Ser mutant had similar ratio of activities with or without potassium (Table II). This result is in agreement with the fact that Gly28 is not directly involved in binding of K^+ or the ligand despite that it is an integral member of the conserved fingerprint sequence Asp26-Gly27-Gly28 (DGG). Therefore, its mutation to Ser may alter the local geometry of the site resulting in a decrease of activity but not the ability to bind potassium ion. Other studied mutants (at Gly27 and Glu159 positions) displayed very low activities and non-significant differences in activities with or without potassium ions. This appears logical regarding the fact that Gly27 and Glu159 contribute to the binding of K^+ and Glu159 also to Hcy substrate. Also, Castro et al[17] showed the Glu159Gln had a K_d that was about 400-fold higher than the WT BHMT as measured using intrinsic fluorescence. The low yields of Gly27Ser and Glu159 mutants (Table II) suggest these residues may be important for protein folding.

CONCLUSION

In conclusion, through the combined use of classical biochemistry, theoretical chemistry, and structural biology our work reveals the dependence of BHMT activity on potassium ions and suggests the structural role of this ion in facilitating binding of Hcy substrate to the BHMT active site. The potassium binding site is composed of Asp26, Gly27, Gln72, Glu159, Gln247 and Gly298 residues, the location of K^+ binding site is identical to that in MS and K^+ binding residues in BHMT partially overlap with the previously identified DGG (Asp26-Gly27-Gly28) fingerprint

in the Pfam 02574 group of methyltransferases. The results presented here provide new important information about the structure of BHMT active site and highlight the effectiveness of joint multidisciplinary approaches, both experimental and theoretical, for solving biological problems.

ACKNOWLEDGEMENTS

This work was supported by the Grant Agency of the Czech Republic (projects P207/10/1277 to JJ and P208/12/G016 to PJ), by the Research Project of the Academy of Sciences of the Czech Republic (RVO: 61388963, to the Institute of Organic Chemistry and Biochemistry), Illinois Agricultural Research Station (ILLU-698-388; to TG), University of Illinois Research Board (12063; to TG) and in part by USUHS start-up grant R071KB (to MK). Support to PJ from the Academy of Sciences (Praemium Academie Award) is gratefully acknowledged. JP also thanks the International Max-Planck Research School for support.

Supporting Information

Additional Supporting Information may be found in the online version of this article.

Accession code

The atomic coordinates and structure factors for human BHMT:L-Hcy structure (PDB code 4M3P) have been deposited in the Protein Data Bank (http://www.rcsb.org/pdb/).

REFERENCES

1. Delgado-Reyes CV, Wallig MA, Garrow TA. Immunohistochemical detection of betaine-homocysteine S-methyltransferase in human, pig, and rat liver and kidney. Arch Biochem Biophys 2001;393:184-186.
2. Petrossian TC, Clarke SG. Uncovering the human methyltransferasome. Mol Cel Proteomics 2011;10:1-12.
3. Park EI, Renduchintala MS, Garrow TA. Diet-induced changes in hepatic betaine-homocysteine methyltransferase activity are mediated by changes in the steady-state level of its mRNA. J Nutr Biochem 1997;8:541-545.
4. Park EI, Garrow TA. Interaction between dietary methionine and methyl donor intake on rat liver betaine-homocysteine methyltransferase gene expression and organization of the human gene. J Biol Chem 1999;274:7816-7824.
5. Delgado-Reyes CV, Garrow TA. High sodium chloride intake decreases betaine-homocysteine methyltransferase expression in guinea pig liver and kidney. Am J Physiol 2005;288:R182-R187.
6. Schafer C, Hoffmann L, Heldt K, Lornejad-Schafer MR, Brauers G, Gehrmann T, Garrow T A, Haussinger D, Mayatepek E, Schwahn BC, Schliess F. Osmotic regulation of betaine homocysteine-S-methyltransferase expression in H4IIE rat hepatoma cells. Am J Physiol 2007;292:G1089-G1098.
7. Fromm HJ, Nordlie RC. On the purification and kinetics of rat liver thetin-homocysteine transmethylase. Arch Biochem Biophys 1959;81:363-376.
8. Finkelstein JD, Harris BJ, Kyle WE. Methionine metabolism in mammals: kinetic study of betaine-homocysteine methyltransferase. Arch Biochem Biophys 1972;153:320-324.

9. Garrow TA. Purification, kinetic properties, and cDNA cloning of mammalian betaine-homocysteine methyltransferase. J Biol Chem 1996;271:22831-22838.
10. Millian NS, Garrow TA. Human betaine-homocysteine methyltransferase is a zinc metalloenzyme. Arch Biochem Biophys 1998;356:93-98.
11. Breksa III AP, Garrow TA. Recombinant human liver betaine-homocysteine S-methyltransferase: identification of three cysteine residues critical for zinc binding. Biochemistry 1999;38:13991-13998.
12. Breksa AP, Garrow TA. Random mutagenesis of the zinc-binding motif of betaine-homocysteine methyltransferase reveals that Gly 214 is essential. Arch Biochem Biophys 2002;399:73-80.
13. Evans JC, Huddler DP, Jiracek J, Castro C, Millian NS, Garrow TA, Ludwig ML. Betaine-homocysteine methyltransferase. Zinc in a distorted barrel. Structure 2002;10:1159-1071.
14. Jiracek J, Collinsova M, Rosenberg I, Budesinsky M, Protivinska E, Netusilova H, Garrow TA. S-alkylated homocysteine derivatives: New inhibitors of human betaine-homocysteine S-methyltransferase. J Med Chem 2006;49:3982-3989.
15. Peariso K, Goulding CW, Huang S, Matthews RG, Penner-Hahn JE. Characterization of the zinc binding site in methionine synthase enzymes of Escherichia coli: The role of zinc in the methylation of homocysteine. J Am Chem Soc 1998;120:8410-8416.
16. Goulding CW, Matthews RG. Cobalamin-dependent methionine synthase from Escherichia coli: involvement of zinc in homocysteine activation. Biochemistry 1997;36:15749-15757.
17. Castro C, Gratson AA, Evans JC, Jiracek J, Collinsova M, Ludwig ML, Garrow TA. Dissecting the catalytic mechanism of betaine-homocysteine S-methyltransferase by use of intrinsic tryptophan fluorescence and site-directed mutagenesis. Biochemistry 2004;43:5341-5351.

18. Gonzalez B, Pajares MA, Martinez-Ripoll M, Blundell TL, Sanz-Aparicio J. Crystal structure of rat liver betaine homocysteine S-methyltransferase reveals new oligomerization features and conformational changes upon substrate binding. J Mol Biol 2004;338:771-782.
19. Vanek V, Budesinsky M, Kabeleova P, Sanda M, Kozisek M, Hanclova I, Mladkova J, Brynda J, Rosenberg I, Koutmos M, Garrow TA, Jiracek J. Structure-activity study of new inhibitors of human betaine-homocysteine S-methyltransferase. J Med Chem 2009;52:3652-3665.
20. Picha J, Vanek V, Budesinsky M, Mladkova J, Garrow TA, Jiracek, J. The development of a new class of inhibitors for betaine-homocysteine S-methyltransferase. Eur J Med Chem 2013;65:256-275.
21. Koutmos M, Pejchal R, Bomer TM, Matthews RG, Smith JL, Ludwig ML. Metal active site elasticity linked to activation of homocysteine in methionine synthases. Proc Natl Acad Sci U S A 2008;105:3286-3291.
22. Mladkova J, Vanek V, Budesinsky MG, Elbert T, Demianova Z, Garrow TA, Jiracek J. Double-headed sulfur-linked amino acids as first inhibitors for betaine-homocysteine S-methyltransferase 2. J Med Chem 2012;55,6822-6831.
23. Bradford MM. A rapid and sensitive method for the quantitation of microgram quantities of protein utilizing the principle of protein-dye binding. Anal Biochem 1976;72:248-254.
24. Bertosa B, Kojic-Prodic B, Wade RC, Tomic S. Mechanism of auxin interaction with auxin binding protein (ABP1): A molecular dynamics simulation study. Biophys J 2008;94:27-37.
25. Klusak V, Barinka C, Plechanovova A, Mlcochova P, Konvalinka J, Rulisek L, Lubkowski, J. Reaction mechanism of glutamate carboxypeptidase II revealed by mutagenesis, X-ray crystallography, and computational methods. Biochemistry 2009;48:4126-4138.
26. Gaussian, Inc., Wallingford CT, U. S. A., Gaussian 09, Revision A.1, 2009.

27. Dudev, T.; Lim, C. Factors governing the protonation state of cysteines in proteins: An ab initio/CDM study. J Am Chem Soc 2002;124:6759-6766.

28. Heyda J, Pokorna J, Vrbka L, Vacha R, Jagoda-Cwiklik B, Konvalinka J, Jungwirth P, Vondrasek J. Ion specific effects of sodium and potassium on the catalytic activity of HIV-1 protease. Phys Chem Chem Phys 2009;11:7599-7604.

29. Jurkiewicz P, Cwiklik L, Vojtiskova A, Jungwirth P, Hof M. Structure, dynamics, and hydration of POPC/POPS bilayers suspended in NaCl, KCl, and CsCl solutions. Biochim Biophys Acta 2012;1818:609-616.

30. Duan Y, Wu C, Chowdhury S, Lee MC, Xiong GM, Zhang W, Yang R, Cieplak P, Luo R, Lee T, Caldwell J, Wang JM, Kollman P. A point-charge force field for molecular mechanics simulations of proteins based on condensed-phase quantum mechanical calculations. J Comput Chem 2003;24:1999-2012.

31. Berendsen HJC, Grigera JR, Straatsma TP. The missing term in effective pair Potentials. J Phys Chem 1987;91:6269-6271.

32. Case DA,, Darden TA, Cheatham III TE, Simmerling CL, Wang J, Duke RE, Luo R, Walker RC, Zhang W, Merz KM., Roberts BP, Wang B, Hayik S, Roitberg A, Seabra G, Kolossvai I, Wong KF, Paesani F, Vanicek J, Liu J, Wu X, Brozell SR, Steinbrecher T, Gohlke H, Cai Q, Ye X, Wang J, Hsieh MJ, Cui G, Roe DR, Mathews DH, Seetin MG, Sagui C, Babin V, Luchko T, Gusarov S, Kovalenko A, Kollman PA, University of California, San Francisco CA, U. S. A., AMBER version 11; University of California, San Francisco, 2010.

33. Heyda J, Kozisek M, Bednarova L, Thompson G, Konvalinka J, Vondrasek J, Jungwirth P. Urea and guanidinium induced denaturation of a trp-cage miniprotein. J Phys Chem B 2011;115:8910-8924.

34. Ryckaert JP, Ciccotti G, Berendsen HJC. Numerical-integration of cartesian equations of motion of a system with constraints - molecular-dynamics of N-alkanes. J Comput Phys 1977;23:327-341.
35. Davies JR, Scopes RK. Purification of some tricarboxylic acid cycle enzymes from beef heart using affinity elution chromatography. Anal Biochem 1981;114:19-27.
36. Berendsen HJC, Postma JPM, Vangunsteren WF, Dinola A, Haak JR. Molecular-dynamics with coupling to an external bath. J Chem Phys 1984;81:3684-3690.
37. Datta S, Koutmos M, Pattridge KA, Ludwig ML, Matthews RG. A disulfide-stabilized conformer of methionine synthase reveals an unexpected role for the histidine ligand of the cobalamin cofactor. Proc Natl Acad Sci U S A 2008;105:4115-4120.
38. Kabsch W. Xds. Acta Crystallogr D 2010;66:125-132.
39. Kissinger CR, Gehlhaar DK, Fogel DB. Rapid automated molecular replacement by evolutionary search. Acta Crystallogr D 1999;55:484-491.
40. Brunger AT, Adams PD, Clore GM, Delano WL, Gros P, Grosse-Kunstleve RW, Jiang JS, Kuszewski J, Nilges M, Pannu NS, Read RJ, Rice LM, Simonson T, Warren GL. Crystallography & NMR system: A new software suite for macromolecular structure determination. Acta Crystallogr D 1998;54:905-921.
41. Murshudov GN, Vagin AA, Dodson EJ. Refinement of macromolecular structures by the maximum-likelihood method. Acta Crystallogr D 1997;53:240-255.
42. Bailey S, Collaborative Computational Project, number 4. The Ccp4 Suite: Programs for Protein Crystallography. Acta Crystallogr D 1994;50:760-763.
43. Emsley, P.; Cowtan, K. Coot: model-building tools for molecular graphics. Acta Crystallogr D 2004;60:2126-2132.

44. Davis IW, Leaver-Fay A, Chen VB, Block JN, Kapral GJ, Wang X, Murray LW, Arendall, WB, Snoeyink J, Richardson JS, Richardson DC. MolProbity: all-atom contacts and structure validation for proteins and nucleic acids. Nucleic Acids Res 2007;35:W375-W383.

45. Skiba WE, Taylor MP, Wells MS, Mangum JH, Awad WM Jr. Human hepatic methionine biosynthesis. Purification and characterization of betaine:homocysteine S-methyltransferase. J Biol Chem 1982;257:14944-14948.

46. Li F, Feng QP, Lee C, Wang SZ, Pelleymounter LL, Moon I, Eckloff BW, Wieben ED, Schaid DJ, Yee V, Weinshilboum RM. Human betaine-homocysteine methyltransferase (BHMT) and BHMT2: Common gene sequence variation and functional characterization. Mol Genet Metab 2008;94:326-335.

47. Page MJ, Di Cera E. Role of Na+ and K+ in enzyme function. Physiol Rev 2006, 86 (4), 1049-1092.

48. Vrbka L, Vondrasek J, Jagoda-Cwiklik B, Vacha R, Jungwirth P. Quantification and rationalization of the higher affinity of sodium over potassium to protein surfaces. Proc Natl Acad Sci U S A 2006;103:15440-15444.

49. Liu HH, Lu P, Guo YY, Farrell E, Zhang X, Zheng M, Bosano B, Zhang, ZM, Allard J, Liao GC, Fu SY, Chen JZ, Dolim K, Kuroda A, Usuka J, Cheng J, Tao W, Welch K, Liu YZ, Pease J, de Keczer SA, Masjedizadeh M, Hu, JS, Weller P, Garrow T, Peltz, G. An integrative genomic analysis identifies Bhmt2 as a diet-dependent genetic factor protecting against acetaminophen-induced liver toxicity. Genome Res 2010;20:28-35.

50. Szegedi, S. S.; Castro, C.; Koutmos, M.; Garrow, T. A. Betaine-homocysteine S-methyltransferase-2 is an S-methylmethionine-homocysteine methyltransferase. J Biol Chem 2008;283:8939-8945.

51. Di Cera E.A structural perspective on enzymes activated by monovalent cations. J Biol Chem 2006;281:1305-1308.
52. Harding MM. Metal-ligand geometry relevant to proteins and in proteins: sodium and potassium. Acta Crystallogr D 2002;58,872-874.

Figure 1. The effects of monovalent cations on BHMT activity for betaine and Hcy. All cations were added as chloride salts and tested at 0 - 400 mM concentrations. KCl is in blue, RbCl is in red, NH_4Cl is in green, NaCl is in violet, LiCl is in brown and CsCl is in black. The data are shown as means of at least tetraplicate measurements ± S.E. V is the velocity of BHMT catalyzed reaction in dpm per h and c_M stands for molar concentration of ions. The data were measured using conditions of standard reaction mixture (250 μM betaine, 100 μM D,L-Hcy) as described in Methods (BHMT activity assays).

Figure 2. Active site representation of a calculated potassium ion density map for a BHMT monomer (dark purple spots) with an isovalue corresponding to a 10-fold the bulk solution concentration of K^+. Panel **A** shows the most prevalent binding sites for potassium ion in the enzyme depleted of the ligand were predicted to localize near the Asp26 and Glu159 residues. Panel **B** shows that in the presence of the CBHcy inhibitor the binding site for potassium shifts closer to Asp26 while Glu159 is no more directly involved. Zinc ion is shown in grey and its ligands, Cys247, Cys299, Cys300 and Tyr160 (panel **A**) or CBHcy inhibitor (panel **B**) are in yellow.

Figure 3. Radial distribution functions (dashed lines) and cumulative numbers of alkali cations (full lines) in the active site of ligand-depleted BHMT containing the two negatively charged residues Asp26 and Glu159 (r is the distance between the carboxylate carbon of Asp26 and the cation).

Figure 4. A detailed view of the modeled potassium ion binding site without (**A**) and with (**B**) the CBHcy inhibitor present in BHMT structure. The closest residues and water molecules are shown

in balls and sticks with the inhibitor in yellow. The potassium cation is depicted in purple and the zinc cation in grey.

Figure 5. Tetramer of BHMT with L-Hcy bound. The individual BHMT monomers are shown in green, red, yellow and blue. K^+ and Zn^{2+} ions shown as spheres are in purple and gray, respectively (spheres not drawn to scale). L-Hcy ligand is shown in sticks.

Figure 6. Electron density map for K^+ binding site in BHMT is shown in panels **A** and **B.** The protein is shown as yellow cartoon with important residues lining the active site and Hcy ligand shown with sticks. Simulated annealing composite omit weighted 2Fobs-Fcalc density map for selected residues and K^+ and Zn^{2+} ions shown in light blue is contoured at 1.5 σ. Electron density map contoured at 7 σ is shown in green in panel **A**, while the same electron density map contoured at 6 σ and 12 σ is shown with green and purple respectively in panel **B**. Water molecules are presented as red spheres. Panels **C** and **D** represent two different views of cartoon representation of the K^+ ion binding site in BHMT rotated by 180°, respectively. Residues that form the K^+ binding site are shown in balls and sticks. The Hcy ligand in proximity to the K^+ ion is drawn in yellow and shown in balls and sticks. The eight-coordinated K^+ ion is shown as purple sphere (spheres are not drawn to scale).

Table I. Values of kinetic constants of human recombinant BHMT toward pairs of its substrates (betaine/D,L-Hcy or SMM/D,L-Hcy) with or without 150 mM potassium ions. The experimental details are provided in Experimental Procedures.

	Without KCl	Without KCl	With 150 mM KCl	With 150 mM KCl	With 150 mM KCl[a]	With 150 mM KCl[a]
	For betaine (at 10 mM D,L-Hcy)	For D,L-Hcy (at 2 mM betaine)	For betaine (at 10 mM D,L-Hcy)	For D,L-Hcy (at 2 mM betaine)	For SMM (at 10 mM D,L-Hcy)	For D,L-Hcy (at 0.25 mM SMM)
K_M (μM)[b]	75 ± 20	338 ± 120	59.4 ± 4.9	15.2 ± 5.7	~ 3,400	~ 2,300
k_{cat} (h^{-1})[b]	107 ± 8	132 ± 13	152 ± 5	136 ± 38	~ 16	~ 1.2
k_{cat} / K_M	1.43	0.39	2.56	8.95	~ 4.7 x 10^{-3}	~ 5.2 x 10^{-4}

[a]The kinetic data determined with SMM have only approximate character due to low enzyme activities under reaction conditions.

[b]Each value represents the mean of ± S.E. of multiple determinations (n = 3).

Table II. Purification yields of WT BHMT and BHMT mutants and their enzymatic activities and binding affinities (K_d for L-Hcy) with or without potassium ions.

Protein	Total yield (mg)	Relative specific activity (%)[a] With potassium	Relative specific activity (%)[a] Without potassium	Ratio of relative specific activities with/without potassium	K_d (μM)[b] with potassium
WT	10	940 ± 22	100 ± 9	9.4	4 ± 2
Asp26Ala	13	18 ± 5	5 ± 0.4	3.7	116 ± 13
Gly27Ser	2	2 ± 1	2 ± 1	0.9	nb
Gly28Ser	15	196 ± 15	26 ± 9	7.6	61 ± 8
Glu159Ala	0.2	na	na	nd	nd
Glu159Gln	0.01	na	na	nd	nd
Glu159Asp	0	nd	nd	nd	nd

[a]Measured at 250 μM betaine (0.3 μCi), 100 μM D,L-Hcy, 50 mM Tris/HCl (pH 7.5), 0.07% (w/v) β-mercaptoethanol and 0.2 μM BHMT with or without 150 mM KCl (standard reaction mixture in Methods). Each value represents the mean ± S.E. of multiple determinations ($n \geq 3$).

[b]Measured towards L-Hcy by changes in BHMT intrinsic fluorescence at 1 mM dimethylglycine in 50 mM Tris/HCl (pH 7.5) and with approximately 10 mM potassium cations. Each value represents the mean ± S.E. of multiple determinations ($n = 3$).

nb - no binding detected, na - no activity detected, nd - not determined.

Figure 1

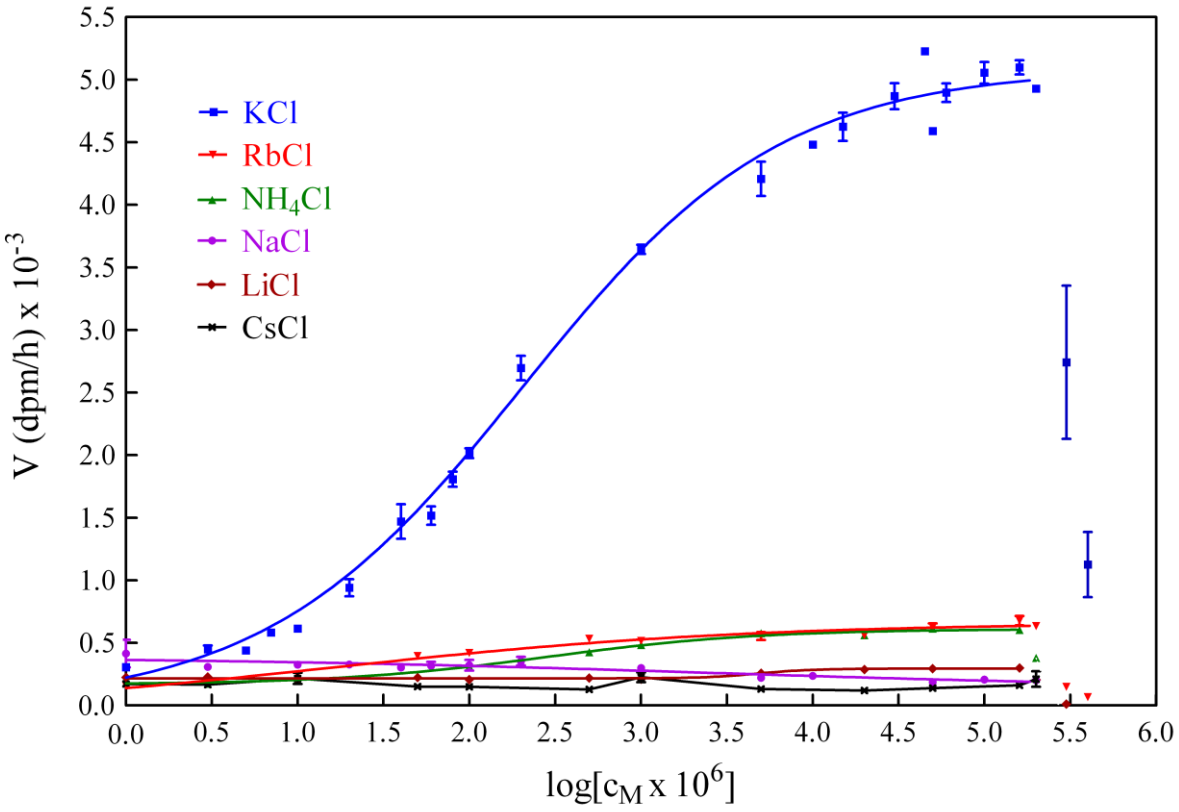
KCl
RbCl
NH4Cl
NaCl
LiCl
CsCl
V (dpm/h) x 10-3
log[cM x 10^6]
0.0
0.5
1.0
1.5
2.0
2.5
3.0
3.5
4.0
4.5
5.0
5.5
6.0

Figure 2

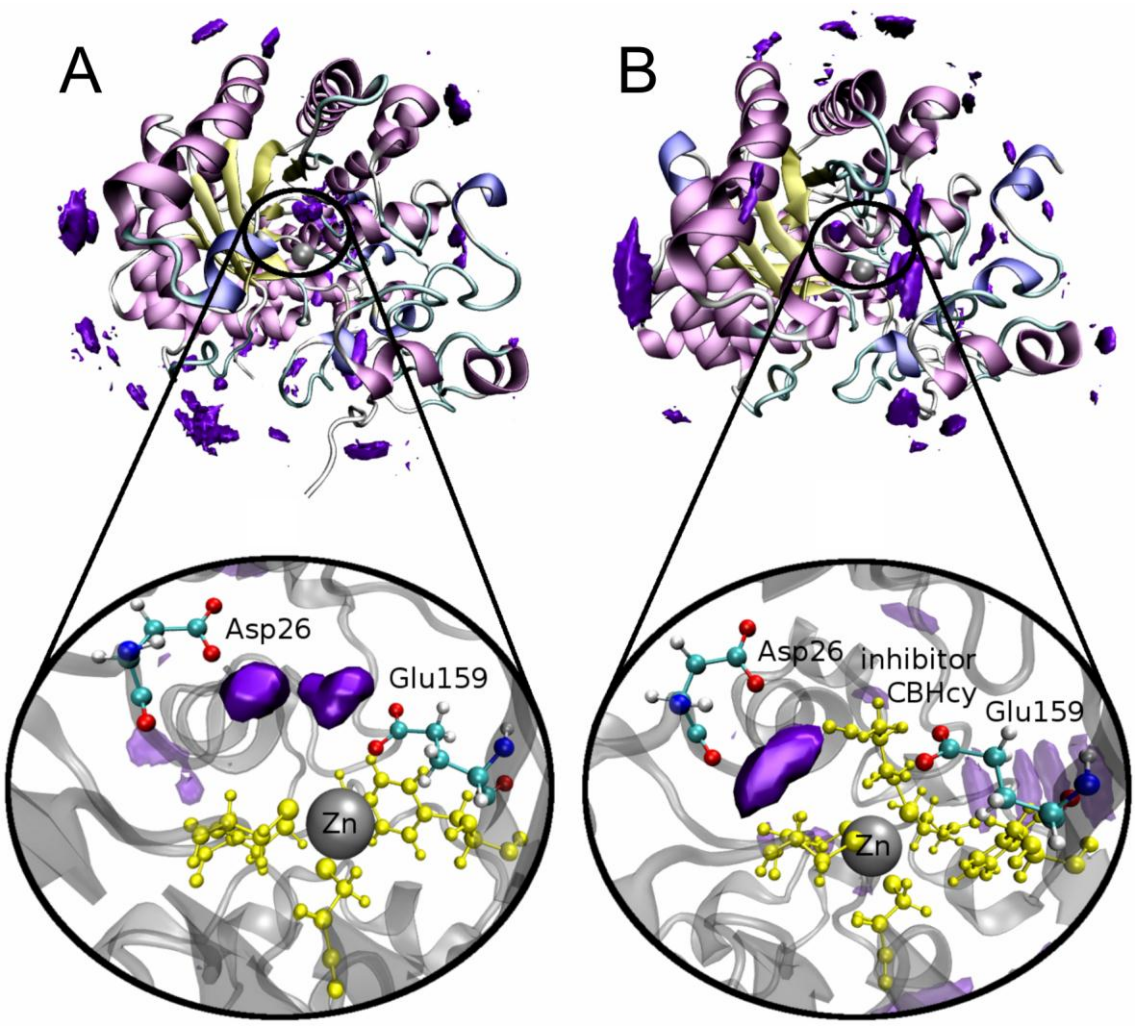

Figure 3

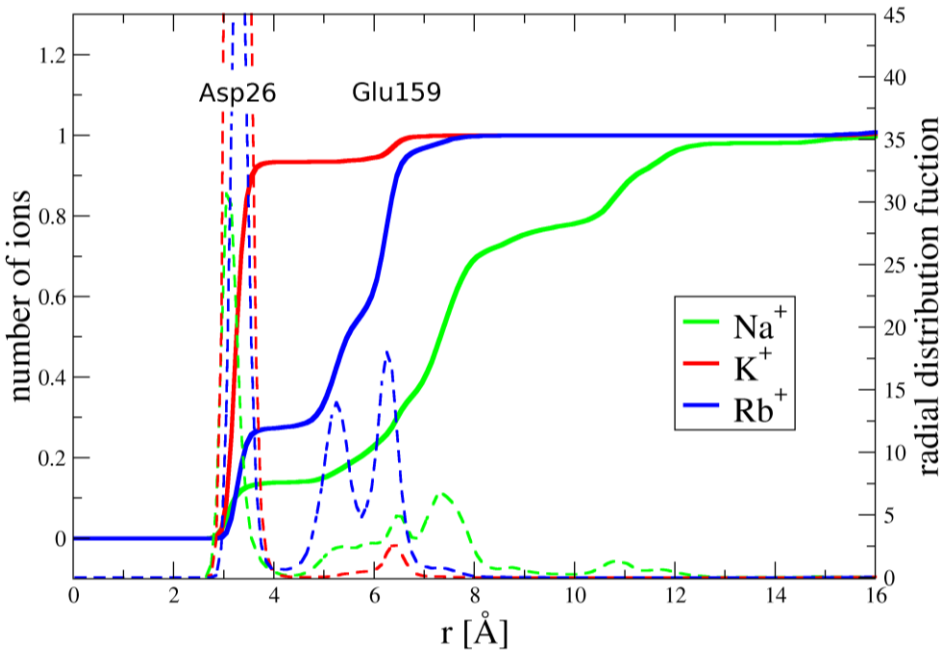

Figure 4

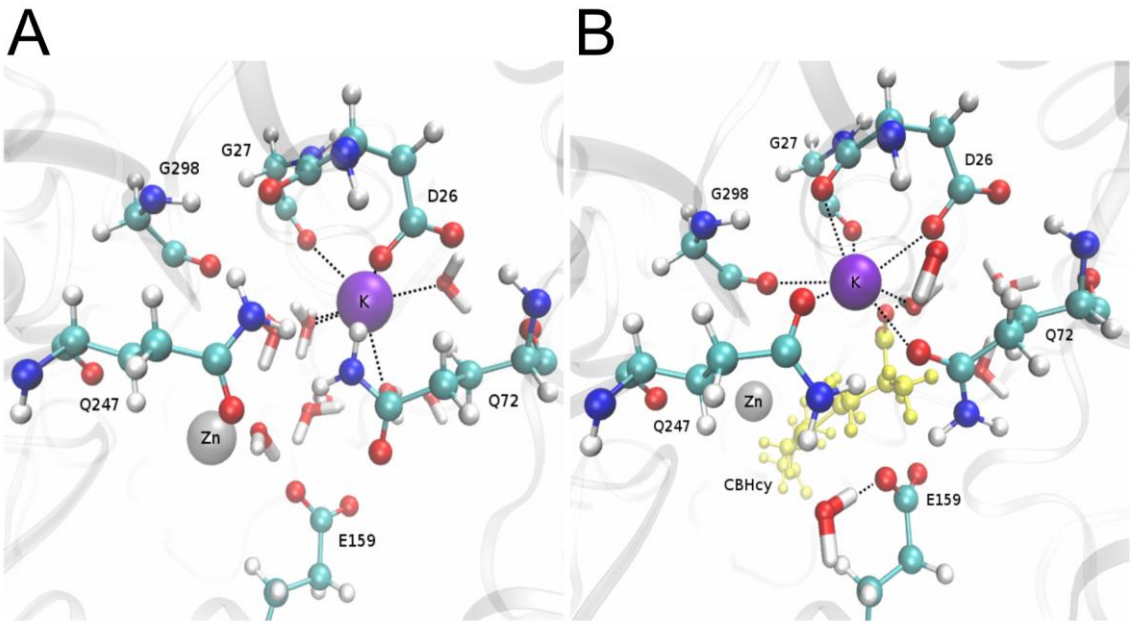

Figure 5

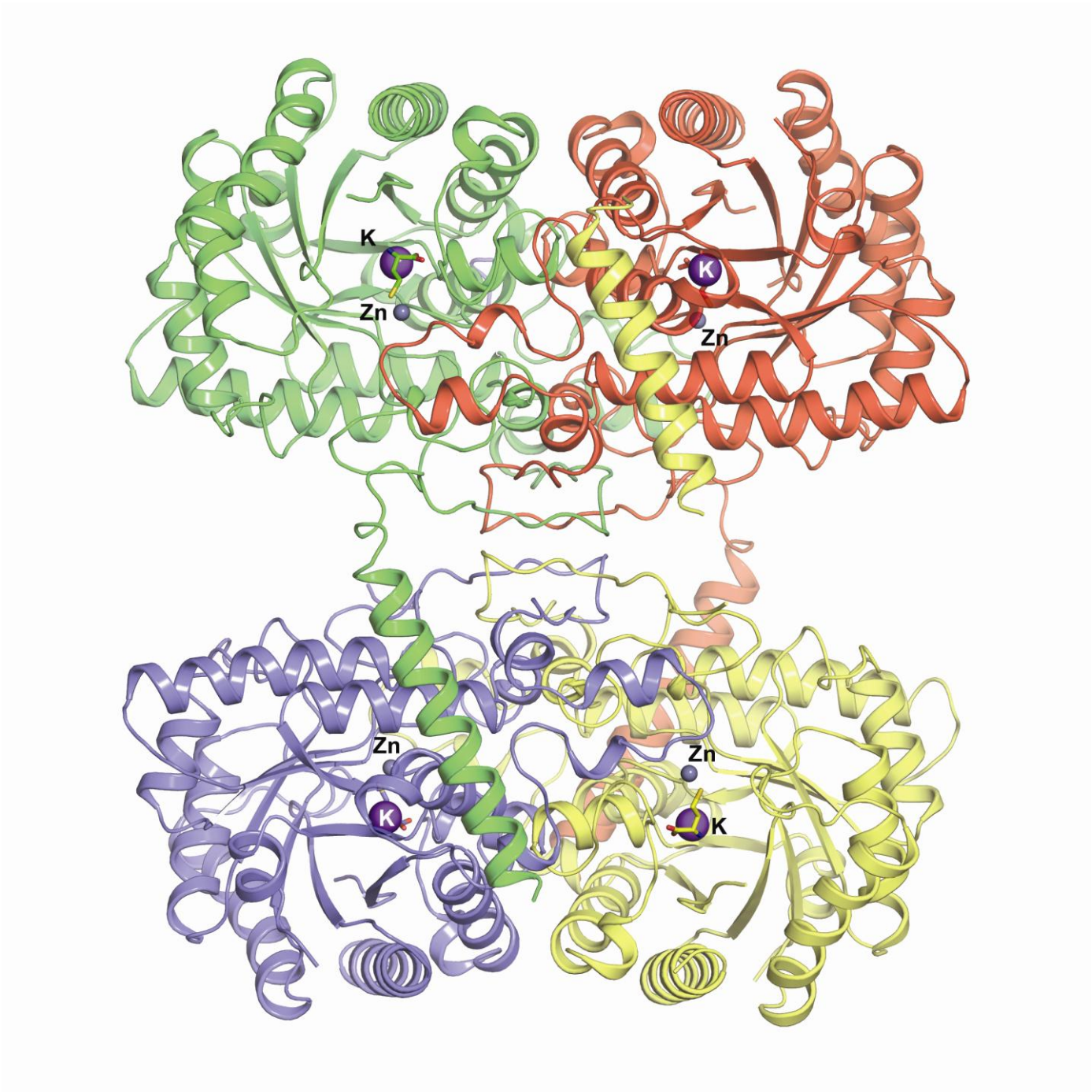

Figure 6

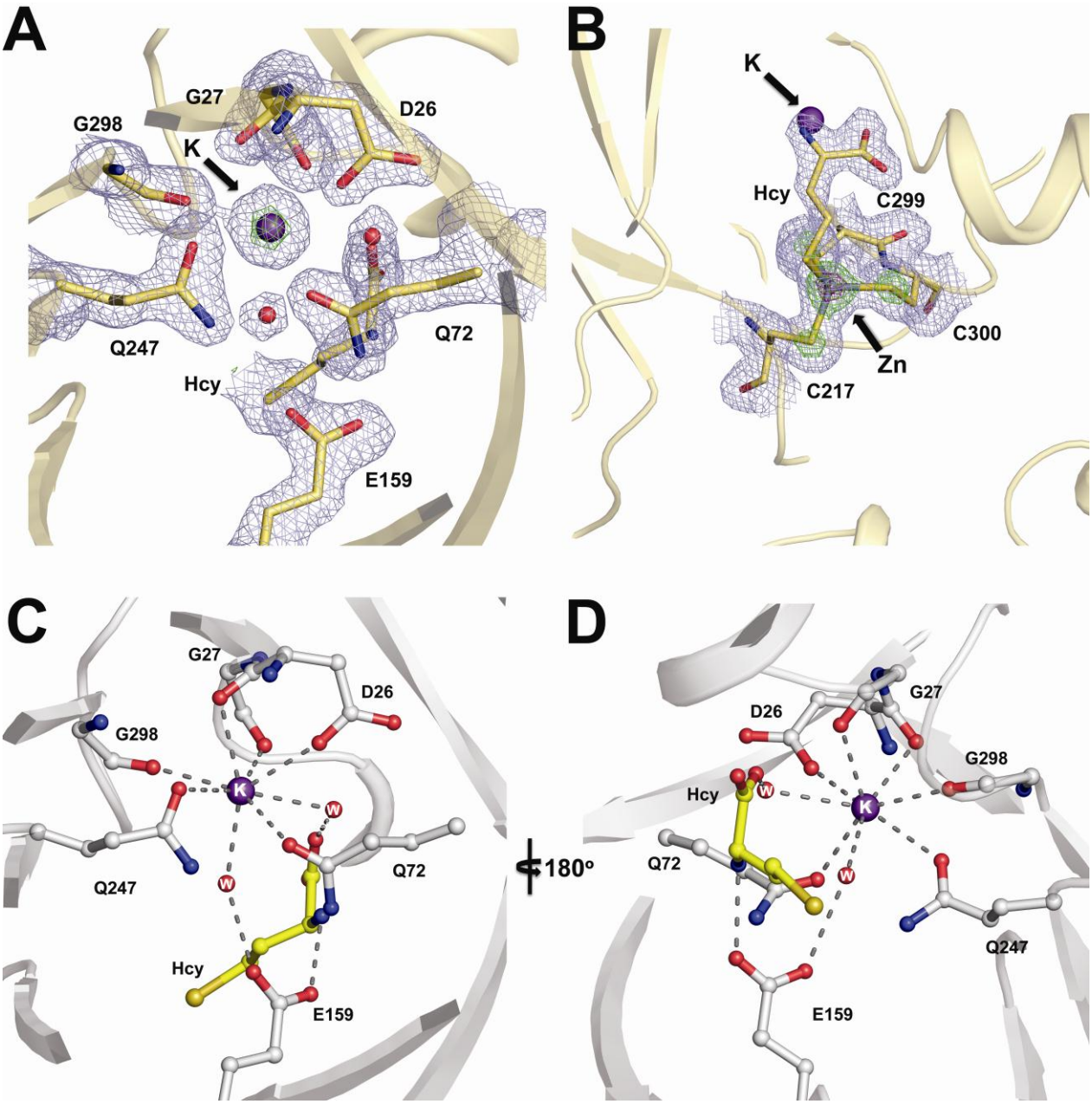
A
G27
D26
G298
K
Q247
Q72
Hcy
E159
B
K
Hcy
C299
C300
Zn
C217
C
G27
D26
G298
K
W
Q247
W
Q72
Hcy
E159
≒180°
D
G27
D26
G298
Hcy
W
K
Q72
W
Q247
E159